CrossMark

Differential expression, distinct localization and opposite effect on Golgi structure and cell differentiation by a novel splice variant of human PRMT5

Muhammad Sohail [a], Manli Zhang [b], David Litchfield [c], Lisheng Wang [d], Sam Kung [b], Jiuyong Xie [a,e,*]

[a] Department of Physiology & Pathophysiology, College of Medicine, Faculty of Health Sciences, University of Manitoba, Winnipeg, MB R3E 0J9, Canada
[b] Department of Immunology, College of Medicine, Faculty of Health Sciences, University of Manitoba, Winnipeg, MB R3E 0J9, Canada
[c] Department of Biochemistry, University of Western Ontario, London, Ontario, Canada
[d] Department of Biochemistry, Microbiology, and Immunology, University of Ottawa, Canada
[e] Department of Biochemistry & Medical Genetics, College of Medicine, Faculty of Health Sciences, University of Manitoba, Winnipeg, MB R3E 0J9, Canada

ARTICLE INFO

ABSTRACT

Alternative splicing contributes greatly to the proteomic diversity of metazoans. Protein arginine methyltransferase 5 (PRMT5) methylates arginines of Golgi components and other factors exerting diverse effects on cell growth/differentiation, but the underlying molecular basis for its subcellular distribution and diverse roles has not been fully understood. Here we show the detailed properties of an evolutionarily emerged splice variant of human PRMT5 (PRMT5S) that is distinct from the original isoform (PRMT5L). The isoforms are differentially expressed among mammalian cells and tissues. The PRMT5S is distributed all over the cell but PRMT5L mainly colocalizes with Giantin, a Golgi marker. PRMT5 knockdown led to an enlarged Giantin pattern, which was prevented by the expression of either isoform. Rescuing PRMT5S also increased the percentage of cells with an interphase Giantin pattern compacted at one end of the nucleus, consistent with its cell cycle-arresting effect, while rescuing PRMT5L increased that of the mitotic Giantin patterns of dynamically fragmented structures. Moreover, the isoforms are differentially expressed during neuronal or dendritic cell differentiation, and their ectopic expression showed an opposite effect on dendritic cell differentiation. Furthermore, besides their differential regulation of gene expression, both isoforms also similarly regulate over a thousand genes particularly those involved in apoptosis and differentiation. Taking these properties together, we propose that their differential expression and subcellular localization contribute to spatial and temporal regulation of arginine methylation and gene expression to exert different effects. The novel PRMT5S likely contributes to the observed diverse effects of PRMT5 in cells.

© 2015 Elsevier B.V. All rights reserved.

1. Introduction

Alternative precursor messenger RNA (pre-mRNA) splicing greatly increases the proteomic diversity in metazoans [1–3]. It is tightly regulated in a spatial and temporal manner [2,4,5]. Mutations that lead to aberrant splicing cause genetic diseases [6,7]. However, the differences between splice variants of many genes that contribute to the proteomic diversity in normal cell function and diseases remain to be characterized.

Protein arginine methyltransferase 5 (PRMT5) catalyzes the symmetric dimethylation of arginines of a diverse group of proteins [8–14], contributing to the regulation of gene expression, snRNP biogenesis, maintenance of stem cell pluripotency and promotion of cell proliferation [9,10,14–19]. The dynamic cytoplasmic or nuclear localization of PRMT5 during early embryonic development is essential for the maintenance of pluripotency or cell fate determination [10]. Particularly in the cytoplasm, PRMT5 is known to localize to the Golgi apparatus (GA) and methylates GM130, a critical factor for Golgi ribbon formation [20]. During mitosis, GA undergoes dynamic structural changes, with a compacted structure near one end of the nucleus in the interphase and various extents of fragmentation during mitosis [21–23]. PRMT5 co-localizes with GA markers and is thought to be required for the maintenance of Golgi structure at interphase through methylation of GM130 [20]. However, the cell cycle-specific structural changes of Golgi due to modulation of cell cycle by PRMT5 have not been considered.

Here we report the detailed properties of a recently identified shorter PRMT5 isoform (PRMT5S) that evolutionarily emerged through exon 3 and partial exon 4 skipping [24,25]. These properties are different from that of the original isoform (PRMT5L), particularly expression among cell lines/tissues, distinct subcellular localization during cell

cycle and its effect on Golgi structure as well as cell differentiation and gene expression.

2. Materials and methods

2.1. RT-PCR

Semi-quantitative RT-PCR of endogenous *PRMT5* was performed as described previously [24,26], using the primer pair hPRMT5F (5′-CAGGAACCTGCTAAGAATCG-3′) and hPRMT5R (5′-GCCAGTGTGGATGT GGTTG-3′). Human tissue-specific total RNA was purchased from Clontech Co. (Cat No. 636643), for which more information can be found at the product page of the company website (http://www.clontech.com). For PCR of *GAPDH* as an RNA loading control, we used the upstream GAPDHF (5′-CTTCATTGACCTCAACTACATGGTT-3′) and downstream GAPDHR (5′-GCTCCTGGAAGATGGTGATG-3′) primers. Both primer pairs are compatible with human, rat or mouse genes.

2.2. Plasmid construction

PRMT5 L or S open reading frames were amplified by PCR from PRMT5 cDNA clone (ID 3833019, OPEN Biosystems) using Phusion High-Fidelity DNA polymerase, and cloned between EcoRI and BglII restriction sites of pCMV-Myc vector. PRMT5L-Flag construct was obtained by cloning the open reading frame along with C-terminal Flag tag between XhoI and ApaI restriction sites of pcDNA3.1 vector. PRMT5 L or S was sub-cloned into vector cppt2E for lentivirus-based expression [27]. The constructs were confirmed by sequencing. We purchased plasmid pLKO.1 containing shRNA against human PRMT5 3′UTR (shPRMT5, clone ID TRCN0000107085, mature antisense sequence TATTCCAGGGAGTTCTTGAGG) from OPEN Biosystems.

2.3. Cell culture and ectopic expression of Myc-PRMT5 isoforms

HeLa and HEK293T cells were cultured and transfected with Myc-tagged PRMT5 plasmids for overexpression as described previously [28]. MDA-MB-231, BT20, U2OS and B35 cells were cultured in DMEM containing 10% fetal bovine serum (FBS) and 1% penicillin/streptomycin/glutamine (PSG) solution (Invitrogen). PC12 cells were grown in DMEM containing 10% horse serum (HS), 2.5% FBS and 1% PSG. GH3 cells were grown in F-10 media containing 10% HS, 2.5% FBS and 1% PSG. H9 cells were obtained from Wicell and approved for use by the local ethics board and the Stem Cell Oversight Committee of the Canadian Institutes of Health Research. These cells were cultured and RNA extracted as described previously [29]. LA-N-5 and MAL (lymphocytes from an ataxia telangiectasia patient [30]) cells were cultured in RPMI containing 10% fetal bovine serum and 1% PSG. For LA-N-5 differentiation, cells were fed with fresh media containing 5 μM 13-*cis*-retinoic acid (RA, R3255, Sigma-Aldrich) every 48 h for 4 days [31–33]. Murine bone marrow-derived dendritic cells (BMDCs) were generated from bone marrow (BM) precursors as previously described [34]. Briefly, mouse BM cells collected from the femura and tibiae were cultured in RPMI 1640 (HyClone) medium containing PSG (Gibco), 2-ME, 10% FBS (HyClone), and 20 ng/ml GM-CSF (PeproTech). Culture medium was changed every 2 days and cells were collected at 7 time points over the course of differentiation for RNA analysis. For ectopic expression of PRMT5L or S in BMDCs, we transduced precursor cells with either one of the protein-expressing viral vectors. Irrelevant EGFP-expressing lentiviral vector (Cppt2E) was used as control [34]. Differentiated DCs with ectopic expression of proteins were fixed and immunostained.

2.4. RNA interference and rescue

For splice variant specific knock down of PRMT5 we synthesized siRNAs targeting PRMT5S-specific sequence TGTCAGGAAGGGCTTTCCT or PRMT5L-specific sequence CTCCATGGATTCGTCCAGA. We transfected HeLa or MDA-MB-231 cells with 360 pmol of siRNA in 6 well plates. Cells were harvested after 60 h of transfection for RNA analysis, immunoprecipitation or immunostaining.

Lentivirus transduction for PRMT5 knock down and rescue with either one of the isoforms was carried out as described [35]. HeLa cells were transduced with shPRMT5-containing virus followed by another transduction along with rescue protein expressing viruses after 36 h. Cells were split and five days after first transduction, harvested for western blot and immunostaining.

2.5. Western blots, immunoprecipitation and immunostaining

Western blots and immunostaining were performed as previously described [36]. Anti-Myc, anti-β-actin, anti-Giantin, anti-PRMT5 (SC2232), anti-PRMT5 (SC136202) and anti-nucleolin were purchased from Santa Cruz Biotechnology Inc. Anti-PRMT5 (EPR5772) was purchased from Abcam, anti-Flag from Sigma and Cy3 conjugated anti-CD40 from Biolegend. For immunostaining, we used primary antibodies at dilution of 1:100 and Texas-Red or FITC conjugated secondary antibodies or Cy3 conjugated CD40 primary antibody at 1:1000. 4′,6-diamidino-2-phenylindole (DAPI) was used at 1:5000 dilution to visualize DNA. Immunoprecipitation was performed as described previously [37], using anti-PRMT5 (EPR5772) and whole cell lysates prepared in radioimmune precipitation assay (RIPA) buffer.

2.6. RNA sequencing

We transfected HEK293T cells with Myc-PRMT5L or -PRMT5S containing plasmids. Total RNA was extracted from triplicates of control (non-transfected) and transfected cells, and submitted to McGill University and Genome Quebec Innovation Centre, where RNA samples were reverse transcribed using random primers for library preparation and subjected to protocols for sequencing using Hiseq 2000/2500 sequencer. We obtained 67 ± 1.9 million uniquely mapped reads on average for each sample. The gene expression analysis was done using DEseq and edgeR [38,39]. We used edgeR-adjusted p values of less than 0.05 for further analysis. For functional clustering of differentially expressed genes we used online tool DAVID 6.7 with the highest stringency and p value < 0.05 [40,41].

3. Results

3.1. Differential expression of PRMT5S in mammalian cells and tissues

In PRMT5S, exon 3 together with the 5′ 46 nt of exon 4 is skipped (Fig. 1A). We measured the PRMT5 variants among cell lines using low cycle number semi-quantitative polymerase chain reaction after reverse transcription (RT-PCR, Fig. 1B). In mRNA transcripts from human cell lines U2OS, HEK293T, MDA-MB-231, HeLa, BT20, H9 and MAL, PRMT5S levels range from 10% (± 2, n = 3, in molar percentage, same as following levels) to 43% (± 3, n = 3) (lanes 2–8). In rat cell lines PC12, B35 and GH₃, no PRMT5S was visible in the agarose gels (lanes 9–11). It was only visible when a more sensitive RT-PCR assay using ^{32}P-labeled primer and denaturing PAGE gels was used (data not shown). Therefore, the PRMT5 variants are differentially expressed among these mammalian cell lines.

To determine the distribution of the novel isoform PRMT5S in humans, we obtained total RNA from 20 different tissues and measured its abundance using semi-quantitative RT-PCR. The result indicates that PRMT5S is differentially expressed among the tissues with varying molar percentages ranging from 8% in the spinal cord to 37% in the kidney (Fig. 1C, lanes 2–21). Cerebellum, testis, thymus and small intestine also have substantial amount of this variant (22–33%, lanes 4, 16, 17 and 20, respectively). This data thus suggests that the expression of PRMT5S is regulated in a tissue-specific manner.
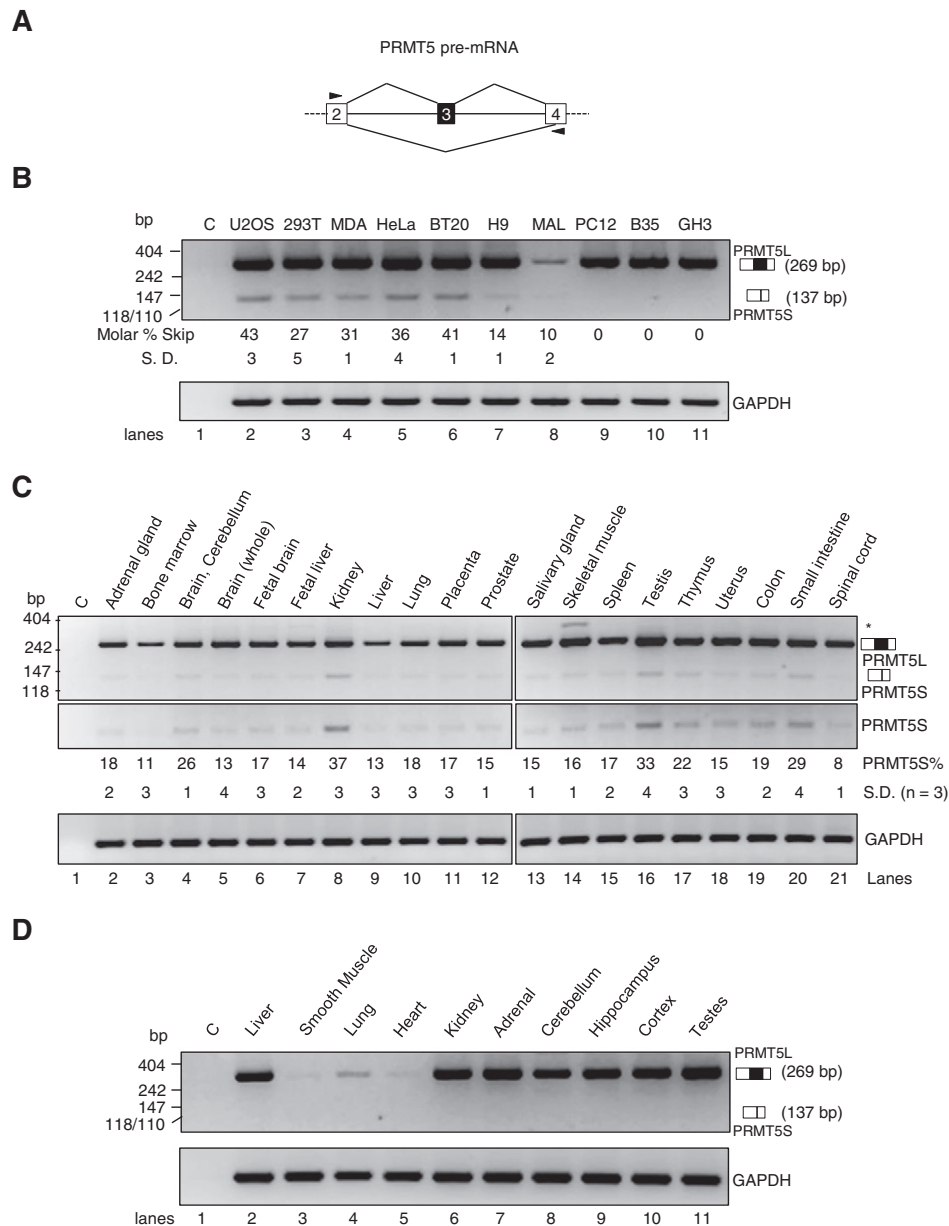
Fig. 1. Differential alternative splicing of PRMT5 exon 3 and 5′ end of exon 4. A, Diagram of PRMT5 pre-mRNA around exon 3 indicating its alternative splicing (not to scale). Arrow heads: positions of PCR primers. B, Differential expression of PRMT5S in mammalian cell lines. Shown are representative images of agarose electrophoresis gels of exon 3 and partial exon 4-included or -excluded RT-PCR products as confirmed by sequencing (lanes 2–11). C (lane 1): PCR control. Human cells: U2OS (osteosarcoma), 293T (embryonic kidney tumor), MDA (breast cancer MDA-MB-231), HeLa (cervical cancer), BT20 (mammary carcinoma), H9 (embryonic stem cells) and MAL (lymphocytes). Rat cells: PC12 (pheochromocytoma), B35 (neuroblastoma) and GH$_3$ (pituitary epithelial-like tumor). C, Differential expression of PRMT5S among 20 human tissues. Upper panel, representative images of agarose electrophoresis gels of semi-quantitative RT-PCR products of PRMT5L or PRMT5S from the 20 human tissues as indicated. Images of the PRMT5S products with longer exposure and higher contrast of the same gels are shown below. The average molar percentages of PRMT5S from three separate PCR reactions are indicated below each lane. Lower panel, RT-PCR products of GAPDH, as an RNA loading control. C: RT-PCR control without reverse transcriptase. *: an unidentified product in skeletal muscle and fetal liver. D, Expression of PRMT5 variants in rat tissues. Shown are images as in B–C of PRMT5 spliced products and GAPDH from different rat tissues (lanes 2–11). C (lane 1): PCR control.

We also examined the expression of PRMT5 variants similarly in ten different rat tissues (Fig. 1D). Consistent with our observations in the above rat cell lines, the PRMT5S in rat tissues was not visible either in agarose gels.

Together these data indicate that PRMT5S is differentially expressed, and is mainly in human cells and tissues.

3.2. Distinct subcellular localization of PRMT5S from that of PRMT5L

To examine the localization of PRMT5 variants, we performed immunostaining experiments. In HeLa cells, Myc-tagged PRMT5L localized mainly around the nucleus, similar to that observed by others [20], while PRMT5S was more diffusely distributed in both the nucleus and cytoplasm (Fig. 2A–B). In HEK293T cells, similar distribution patterns and differences were observed for the expressed variants (Fig. 2B). Therefore their differential subcellular distribution is consistent between the two different types of cells.

The localization of exogenous Myc-PRMT5L also overlaps with a PRMT5L that is Flag-tagged at the COOH-terminus, when co-expressed and -immunostained with the respective tag antibodies in the same HeLa cells (Fig. 2C). Therefore, the punctate distribution of the Myc-PRMT5L is a property of the PRMT5L protein rather than that of the peptide tags used.

A

B

25µm

C

25µm
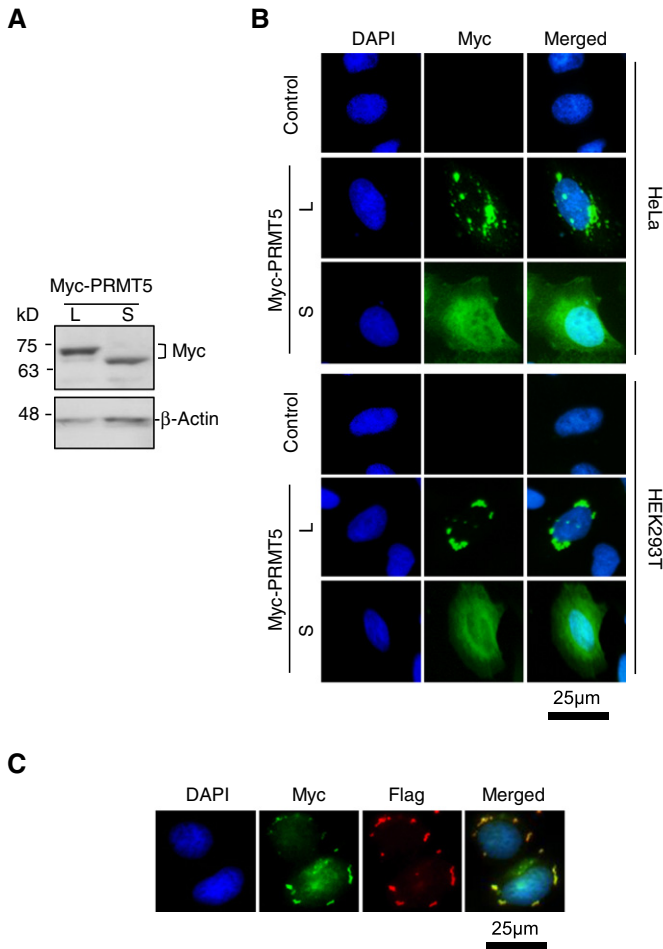
Fig. 2. Expression and intracellular localization of exogenous PRMT5 isoforms. A, Expression of exogenous Myc-PRMT5L or S in HeLa cells. Western blot of HeLa cell lysates transfected with Myc-PRMT5L or S showing the expression of either one of the isoforms. B, Intracellular localization of exogenous PRMT5 isoforms. Shown are immunostained HeLa (upper panel) or HEK293T (lower panel) cells transfected as in A, using anti-Myc. DAPI staining of nuclei is merged with the Myc signals in the last column. Non-transfected control cells are shown in the top row of each panel. C, Subcellular localization of exogenous PRMT5 containing a different tag. Shown are HeLa cells co-transfected with Myc- or Flag-tagged PRMT5 and immunostained using anti-Myc or anti-Flag. DAPI staining of nuclei, Flag and Myc signal are merged in the last image.

To verify the localization of endogenous PRMT5 isoforms, we carried out splice variant-specific RNA interference using siRNAs targeting exon 3 (PRMT5L-specific) or the junction of exons 2 and 4 (PRMT5S-specific). We transfected HeLa cells with scrambled or either of the splice variant specific siRNAs. These PRMT5 siRNAs decreased the level of specific target transcripts as verified by RT-PCR, from 33% to 6% for PRMT5S (Fig. 3A, lower band, $p = 2.1E-6$, n = 3, lane 3 compared to lane 2) and from 67% to 39% for PRMT5L (upper band, $p = 1.5E-4$, n = 3, lane 4 compared to lane 2). Thus, the siRNAs specifically reduced either one of the endogenous PRMT5 variants.

To confirm the variant-specific knockdown of endogenous proteins, we carried out western blots of immunoprecipitated PRMT5 from protein lysates of siRNA-transfected HeLa or MDA-MB-231 cells. Consistent changes were observed in both cell samples but the MDA sample showed a slightly higher relative level of PRMT5S-like band in the assay (Fig. 3B). The PRMT5L-specific siRNA decreased the ratio of PRMT5L/S-like from 3.5 to 2.2 (lane 3 compared to lane 2) whereas PRMT5S-specific siRNA increased the ratio to 5.1 in the MDA cells (lane 4 compared to lanes 2 and 3). Thus, the ratio of the protein isoforms change consistently as the mRNA variants upon variant-specific

siRNA knockdown, supporting the identity of the PRMT5S-like band as endogenous PRMT5S protein in cells.

We next examined the localization of endogenous PRMT5 in HeLa cells by immunostaining of the remaining isoforms (Fig. 3C). In most of the control siRNA-transfected cells (91% ±2.5%, n = 3 groups, 100 cells each group, same in the following localization analysis in this figure), the endogenous PRMT5 staining pattern showed punctate spots with light diffusing backgrounds (Fig. 3C, siC panel), consistent with the presence of both the long and short isoforms. Transfection of PRMT5L-specific siRNA significantly reduced the number of strong spots and led to more diffuse distribution in about 59% (±4%, n = 3 groups) of cells (Fig. 3C, siPRMT5L panel). In contrast, transfection of PRMT5S-specific siRNA created bright spots and simultaneously reduced the diffusing backgrounds in 68% (±3%, n = 3 groups) of cells (Fig. 3, siPRMT5S panel). These changes were also confirmed by immunostaining with a different PRMT5 antibody under higher magnification (Fig. 3D), with the siPRMT5L reducing the punctate staining and siPRMT5S reducing the diffusing staining signals from the control siRNA samples. Thus, the localization changes of endogenous PRMT5 isoforms after splice variant-specific knockdown are consistent with the differences between the Myc-PRMT5 isoforms.

Together, these data support that the exogenous and endogenous PRMT5 isoforms exhibit consistently different subcellular localization. Specifically, the PRMT5S localizes all over the cell, distinct from the highly punctate localization of the PRMT5L.

3.3. PRMT5S has an opposite effect on Golgi structure during cell cycle

The distribution of PRMT5L mainly around the nucleus has been shown to colocalize with the Golgi markers P230, ManII, GM130, NSF, GRASP55 and Giantin, and it methylates GM130 to regulate Golgi structure [20]. The Golgi marker localization is cell cycle-dependent, changing from a compacted structure beside one end of the nucleus in interphase to dynamic fragmented structures during mitosis [21–23, 42,43]. Moreover, PRMT5L itself also promotes mitosis [12,18,19]. We thus examined the localization of the PRMT5S and PRMT5L relative to Giantin during cell cycle in HeLa cells without or with PRMT5 knockdown/rescue to dissect the relationship between the PRMT5 isoforms and Golgi structures (Fig. 4A).

The endogenous PRMT5 exhibited cell cycle-dependent changes in subcellular localization (Fig. 4B, upper/control panel). Particularly the bright areas overlap with Giantin. Interestingly, PRMT5 knockdown resulted in a 1.6 fold (±0.1) increase in the area of the compact Giantin staining in the interphase as compared to that in control cells (p = 2.6E−06, n = 3 experiments, 300 cells each experiment, Fig. 4B, 2nd/shPRMT5 panel). The knockdown also promoted more diffusing distribution of Giantin at metaphase and to a lesser extent at subsequent stages. PRMT5 thus appears to be essential for the compactness of the Golgi apparatus during cell cycle.

In PRMT5 knockdown cells expressing the rescue isoforms, Myc-PRMT5L showed dynamic patterns of localization during cell cycle (Fig. 4B, 3rd panel, shPRMT5 + MycPRMT5L). This pattern overlaps mostly with that of Giantin. In contrast, the Myc-PRMT5S is more homogenously distributed all over the cell during cell cycle (Fig. 4B, bottom panel, shPRMT5 + MycPRMT5S), with its brightest areas overlapping with Giantin as well. Moreover, both rescuing isoforms eliminated the slight changes by PRMT5 knockdown and restored the compactness of the Golgi structures similar to that of the control cells.

Together, the knockdown/rescue data indicate that the PRMT5 isoforms show distinct and dynamic co-localization with the Golgi marker Giantin during cell cycle and they are likely required for the compactness of Golgi structure.

We next examined the effect of PRMT5 isoforms on the prevalence of cells containing interphase compacted or mitotic dynamic Golgi structures. In overexpression experiments, MycPRMT5L increased the
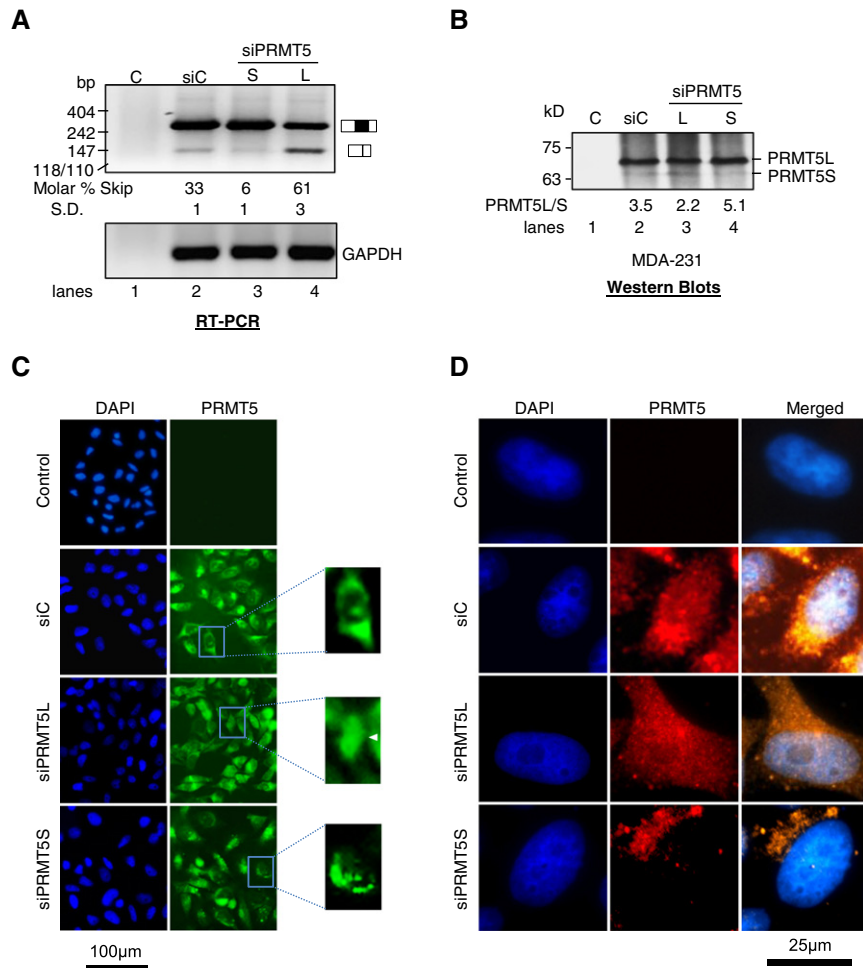
Fig. 3. Differential subcellular localization of endogenous PRMT5 isoforms based on splice variant-specific RNA interference and immunostaining. A, Effect of splice variant-specific knock-down on endogenous PRMT5 variants. Shown are representative images of agarose electrophoresis gels of RT-PCR products of endogenous PRMT5 variants or GAPDH from HeLa cells transfected with scrambled control siRNA (siC) or splice variant-specific siRNA (lanes 2–4). C (lane 1): PCR control. B, Effect of splice variant-specific knockdown on endogenous PRMT5 protein isoforms. Shown is the western blot of immunoprecipitated PRMT5 from MDA-MB-231 cells transfected as in A (lanes 2–4). PRMT5 bands were not detectable in immunoprecipitation controls without PRMT5 antibody (lane 1). C, Effect of splice variant-specific knock-down on endogenous PRMT5 localization. Shown are representative images of HeLa cells transfected with control or PRMT5 splice variant-specific siRNAs and immunostained using anti-PRMT5 (SC136202). Control cells without PRMT5 antibody are shown in the top row. Enlarged pictures of the PRMT5 signals of example cells are in the right column and pointed by a white arrow head in the panel with multiple cells. Nuclei stained with DAPI are in the left column. D, Representative higher magnification images of HeLa cells transfected as in C and immunostained with anti-PRMT5 (SC22132). DAPI-stained nuclei are merged with PRMT5 signal in the right column. Control cells without PRMT5 antibody are shown in the top row.

percentage of cells with mitotic Golgi whereas MycPRMT5S had the opposite effect (Fig. 4C, left panel). Knock-down of endogenous PRMT5 increased the percentage of cells with interphase compact Golgi from 43.5% to 63.2% ($\pm$ 4.6%, p = 0.008, n = 3, 300 cells each, same in the following analysis of Golgi structures in this figure). Rescue with MycPRMT5S further increased this cell population to 76.4% ($\pm$ 5.5%, p = 0.002). In contrast, rescue with MycPRMT5L had the opposite effect: it decreased this cell population to 29.5% ($\pm$ 3.9%, p = 0.02) (Fig. 4C, right panel). These observations are consistent with the opposite effects of the PRMT5 isoforms on mitosis [12,18,19,25]. Thus, PRMT5S has an opposite effect on the number of cells with interphase or mitotic Golgi structure compared to PRMT5L.

3.4. PRMT5 isoforms are differentially expressed during differentiation and PRMT5S has an opposite effect on the differentiation of dendritic cells

The differential expression, localization and effect on cell cycle and Golgi structure suggest that the two isoforms may have more downstream effects on cells. We then explored the role of the PRMT5 isoforms during cell differentiation.

We induced LA-N-5 human neuroblastoma cells differentiation using 13-cis-retinoic acid (RA), as reported by others [31–33]. Upon differentiation, the percentages of exon skipping significantly decreased from 46% to 34% (Fig. 5A–B, p = 0.003, n = 3). Thus, PRMT5 variants are differentially regulated during neuronal differentiation.

We also examined the expression of the variants in mouse dendritic cells (DCs). DCs are derived from hematopoietic stem cells, which undergo tightly regulated lineage commitment, differentiation and maturation processes in vivo [44–46]. In vitro, a well-established culture condition has been used to generate dendritic cells from adherent bone marrow cells in the presence of GM-CSF cytokine [34]. We used the in vitro differentiating DCs as a primary cell model to examine expression of the PRMT5 isoforms. The bone marrow precursor cells did not express any PRMT5 isoform (Fig. 5C, lane 2), while differentiating DCs started to express detectable PRMT5L only on day 3 and at higher levels during the following days (Fig. 5C, lanes 5–7). This suggests that PRMT5 is expressed in a variant-specific and differentiation time-dependent manner in DCs.

We then used this in vitro differentiation system to examine the effect of ectopic expression of either one of the MycPRMT5 isoforms on the differentiation/maturation of DCs. The precursor cells were
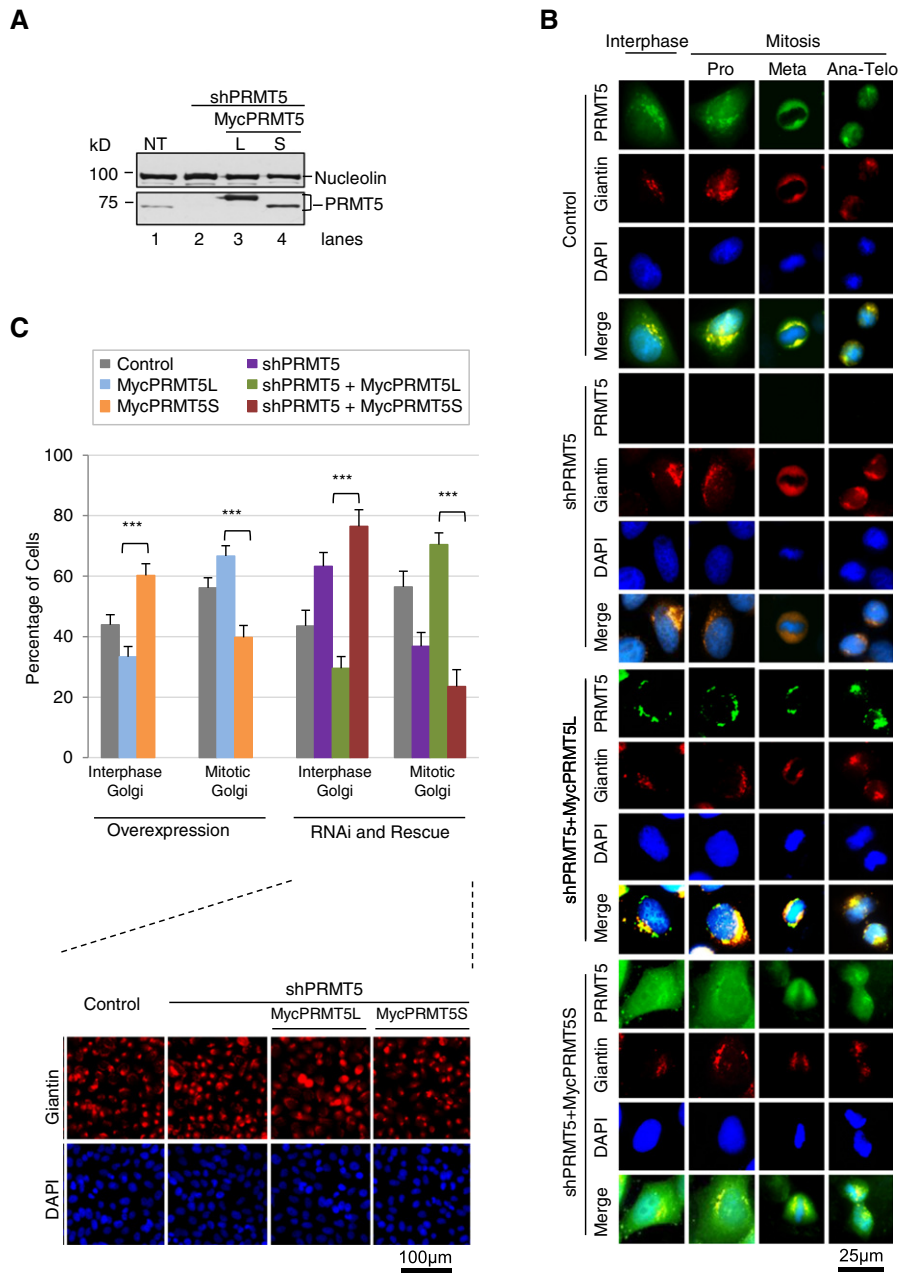
Fig. 4. Colocalization of PRMT5 isoforms with cell cycle-specific Golgi patterns and effects on their structure and prevalence. A, Western blot showing the knock down of endogenous PRMT5 and rescue with PRMT5L or S in HeLa cells using lentiviral transduction of shRNA and expression plasmids. B, Representative images of HeLa cells treated as in A and immuno-stained using anti-PRMT5 (EPR5772) and anti-Giantin at different stages of cell cycle. DAPI-stained nuclei are merged with PRMT5 and Giantin signals in the bottom row of each panel. Pro: Prophase; Meta: Metaphase; Ana–Telo: Anaphase to Telophase. C, Bar graph showing the percentages of HeLa cells with interphase or mitotic Giantin patterns. Interphase: Polarized Giantin beside one end of nucleus; Mitotic: Half circle ribbon, diffused circle or bipolar Giantin representative of later mitosis stages. Left panel shows the percentages of HeLa cells overexpressing either one of the PRMT5 isoforms. Right panel: knockdown/rescue cells treated as in A. ***: $p < 0.001$. Below are the representative images of HeLa cells treated as in A and immunostained with Giantin antibody.

transduced to express the irrelevant EGFP protein, PRMT5S or PRMT5L during the *in vitro* differentiation of DCs, which was defined by the expression of CD40. Non-transduced and mock-transduced cells showed about 10% CD40 positive cells while the PRMT5L-transduced cells showed only 6% CD40 positive cells ($\pm 1.7\%$, $p = 0.01$, n = 3 groups, 300 cells/group, same in the following analysis of CD40). In contrast, the PRMT5S-transduced cells showed about two-fold increase ($\pm 2.5\%$, $p = 8.4E-05$) of CD40 positive cells as compared to controls (Fig. 5D–E). Thus, ectopic expression of the PRMT5S variant in precursor cells promotes the differentiation of DCs, while PRMT5L inhibits it.

3.5. PRMT5 isoforms regulate genes involved in various cellular processes including apoptosis and differentiation

In our recently reported RNAseq data, we have showed that the two isoforms differentially regulate a group of genes including cell cycle-arresting genes preferentially regulated by PRMTS to promote cell cycle arrest whereas PRMT5L promotes mitosis [25]. To identify genes that are similarly regulated by both isoforms, we analyzed further the RNAseq data and identified 1636 genes in HEK293T cells expressing either isoforms with significant difference of the number of reads from the control sample ($p < 0.05$). The number of reads of
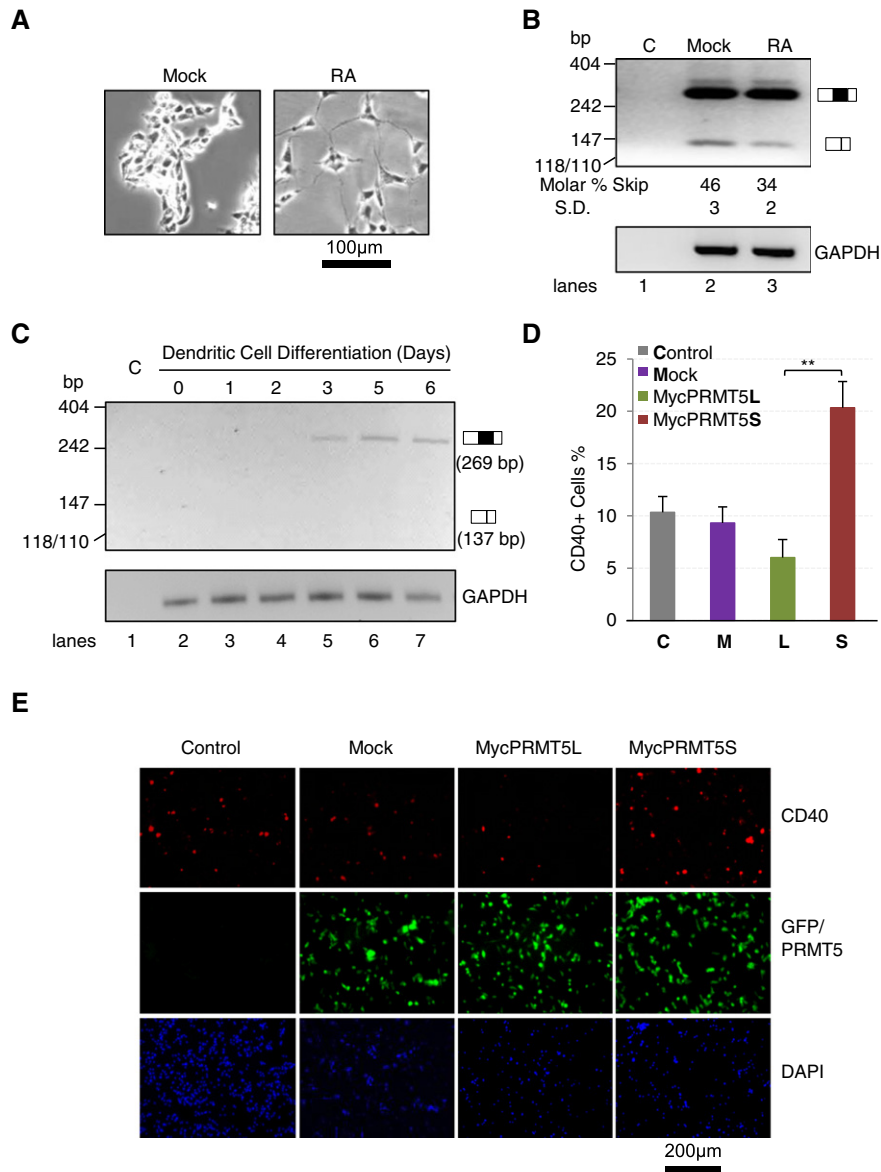
Fig. 5. Differential expression and an opposite effect of PRMT5 isoforms on dendritic cell differentiation. A, Representative images of undifferentiated and differentiated LA-N-5 cells. Shown are Mock or 13-*cis*-retinoic acid (RA)-treated cells. B, Agarose gel electrophoresis images of semi-quantitative RT-PCR products of PRMT5 splice variants and GAPDH in undifferentiated or differentiated LA-N-5 cells (lanes 2, 3). C (lane 1): PCR control. C, Expression of PRMT5 in differentiating dendritic cells. Shown are agarose gel electrophoresis images of RT-PCR products of PRMT5 and GAPDH from precursors at day 0 (lane 2), or following days of differentiation into dendritic cells (lanes 3–7). C (lane 1): PCR control. D, Bar graph showing the percentages of CD40 positive control (non-transduced), mock, PRMT5L or S transduced dendritic cells. **: p < 0.01. E, Representative images of differentiated dendritic cells treated as in D and immunostained with anti-Myc and anti-CD40.

1070 genes was increased whereas 566 genes decreased, suggesting that methylation by PRMT5 could either enhance or inhibit the expression of target genes.

We tested the expression of 25 genes by RT-PCR. Of the 22 genes with correct PCR products, all were confirmed to have the same direction of changes as predicted by the reads from RNAseq analysis [25]. We used the minimal number of reads detectable by RT-PCR (42.4 on average, of 9 samples) as a cut-off value, which resulted in 1072 genes with at least 42 reads. We used these genes for functional clustering analysis using DAVID [40].

These regulated genes cluster most significantly for six functions: homeobox, phosphorylation, differentiation, apoptosis, axonogenesis and transcription (Table 1). For instance, 38 genes including *BCL2* (B-cell lymphoma 2) and *CASP10* (Caspase 10, apoptosis-related cysteine peptidase) in apoptosis and 21 genes including *NRXN3* (Neurxin-3-alpha) and

SLIT2 (Slit homolog 2 protein) in axongenesis. Other functions related to the DC differentiation include innate immune response (p = 0.01) and semaphorins (p = 0.01). For example, the Semaphorin family of genes SEMA3A, D, E, G, and 6D are down-regulated by the PRMT5 isoforms. Interestingly, SEMA4D, which is required for the maturation of dendritic cells [47,48], is up-regulated by 1.5 times (± 0.1, n = 3, p = 0.02). These clusters are consistent with the diverse functions of PRMT5 in cell growth/mitosis and differentiation [9,10,14–19]. Therefore, the control of the expression of genes of different pathways by PRMT5 is likely part of a program of changes underlying its effect on cell properties. While the differentially regulated target genes by the two PRMT5 isoforms may contribute to their differential effects on cell mitosis and differentiation [25], the commonly regulated ones perhaps contribute to the control of common targets in cellular processes such as the dynamic changes of Golgi structure and differentiation.

Table 1
Functional Clustering of genes commonly regulated by PRMT5L and PRMT5S. Genes with well-known functions in their category are highlighted in bold.

Category	p-Value	Genes	# of genes
Homeobox	.0003	POU6F1, HOXA13, PRRX1, ZEB2, PAX3, PDX1, HDX, HOXA3, LHX2, HLX, HOXA6, POU2F2, HOXA10, POU3F2, TLX3, BARHL2, ISL1, HOXD9, HOXB4, DLX1, MSX1, HOXB8, HOXB5, HOPX, HMX3	25
Phosphorylation	.0004	HMGCR, PDGFA, CSF1, TGFB3, TRIB3, PRDX2, ZEB2, BDKRB2, KIT, TRIB2, LATS2, SPRY4, IL11, LIF, SPRY2, DUSP19, NOD2, CDKN2B, BCL2, DUSP16, SPRED2, RAPGEF3, FAM129A, PPP1R14C, FRS2, MAP2K6, PPP1R14A, GHR, BCL10, SPHK1, PIM1, CDK5, CDC25A, PROK2, CDKN1A, CCND1, CNTF, CCND2, GADD45G, IL12A, DUSP8, GADD45A	42
Differentiation	.0009	S100A4, FGF19, ALDH1A2, RET, BCL2, CYP26A1, ZEB2, PAX3, ISL1, GDNF	10
Apoptosis	.001	PTGS2, HOXA13, ZMAT3, APH1B, TGFB3, SMNDC1, PCBP4, SQSTM1, AEN, **BCL2**, TICAM1, TNFRSF19, BCL3, INPP5D, RARB, PHLDA3, FOSL1, DEDD2, MAP2K6, KCNMA1, BCL10, AIFM2, KLF10, NR4A1, CDK5, DDIT3, **CASP10**, CDKN1A, EPHA7, NME3, BBC3, ENDOG, UBC, IL12A, RIPK2, NGFR, DCUN1D3, TP53INP1	38
Axonogenesis	.001	RAB3A, **NRXN3**, ISL1, CDK5, CXCL12, **SLIT2**, NUMBL, EPHA4, EPHA7, UNC5A, LHX2, BCL2, UBC, ROBO2, VCAN, SEMA3A, NGFR, UNC5C, SLITRK5, ETV4, GFRA3	21
Transcription	.001	IRAK2, PTHLH, NOD2, ID1, PIM1, PRDX2, CAT, PROX1, DDIT3	9

4. Discussion

PRMT5 is known to have diverse functions in both the cytoplasm and nucleus in cells but the source of this functional diversity has not been fully understood. Our data demonstrate that PRMT5 isoforms created by exon 3/4 alternative splicing are differentially expressed among different cells and during differentiation. They also exhibit distinct subcellular localization and control the compactness of the Golgi apparatus during cell cycle. Moreover, these two isoforms show opposite effects on prevalence of mitotic Golgi and dendritic cell differentiation, perhaps involving the control of the expression of a group of genes.

PRMT5 has complex roles in cells. For instance, it maintains embryonic stem cell pluripotency during development [10,17], but on the other hand also controls the expression of critical genes in erythroid differentiation [49]. These seemingly opposite processes are thought to be carried out by the same PRMT5 protein. The discovery of the PRMT5S and its distinct properties from PRMT5L makes it worthwhile to explore the presence and potential role of this novel variant in these cellular processes.

PRMT5S contains the intact methyltransferase domain, which is consistent with its capability to maintain methylation of histone 4, a PRMT5 target [25]; however, its skipped region corresponds to a part of N-terminal TIM barrel domain, which interacts with MEP50, a cofactor of PRMT5 [25,50]. The interaction with MEP50 can mediate both substrate recognition and regulation of methyltransferase efficiency of PRMT5 [50–53]. Structural insights into PRMT5 particularly in complex with MEP50 indicate that the PRMT5S-skipped region is located in close proximity to the interface of these proteins [51,52,54]. Besides MEP50, the N-terminal region of PRMT5 is also involved in interactions with RioK1, pIClⁿ and Menin which can modulate PRMT5 activity and substrate specificity [50,55,56]. Therefore, altered interactions of PRMT5S with these proteins can contribute to the differential properties and functional consequences of this variant. Moreover, the N-terminal region of PRMT5 seems to harbor non-canonical nuclear exclusion signals [57], likely disrupted in PRMT5S resulting in a distinct diffusing localization pattern (Figs. 2–4). Interestingly, PRMT5 exhibits subcellular localization-specific effects in several cell types [10,57–62]. Thus, the position of the region skipped in PRMT5S could potentially affect the protein–protein interaction, enzyme efficiency and subcellular localization of this variant leading to differential functional consequences. It'd be interesting to explore if the PRMT5S properties could help explain at least some of the diverse effects of PRMT5 in cells observed previously.

The role of PRMT5 in maintaining the compactness of Golgi structures is supported by the increased area of Golgi marker Giantin at interphase and more diffusing distribution during mitosis upon PRMT5 knock-down (Fig. 4B). This role is carried out by either of the PRMT5 isoforms with a similar effect (Fig. 4B). Besides their common effect on the compactness of the Golgi apparatus, the PRMT5 isoforms also exhibited opposite effects on the distribution of Golgi structures specific for the different phases of cell cycle. We observed the increase of interphase

Golgi structures compacted near one end of the nucleus upon PRMT5 knockdown in cells expressing mainly PRMT5L (Figs. 3–4). Interestingly in rescuing experiments, the two PRMT5 isoforms have opposite effects on the percentage of the interphase/mitotic Golgi structures (Fig. 4), though they both have protein methylation capability [25]. The different effects are consistent with the increase of the percentage of interphase cells by PRMT5S and mitotic cells by PRMT5L, likely through their differential control of a group of genes involved in cell cycle arrest in similar experiments [25].

The presence of PRMT5S all over the cells indicates that it might be a better candidate for the methylation of nuclear proteins such as histones and p53 [9,13,19], as well as cytoplasmic proteins outside of the Golgi apparatus [11,63,64].

In summary, we show here that the two PRMT5 variants have distinct expression, localization and effects on Golgi structure and function in cell differentiation. This adds to the repertoire of PRMT proteins by providing a variant candidate for the diverse and often complex effect of PRMT5 in cells.

Statement of conflict of interest

The authors declare no conflict of interest whatsoever related to this submitted manuscript.

Acknowledgments

References

[1] T. Maniatis, B. Tasic, Alternative pre-mRNA splicing and proteome expansion in metazoans, Nature 418 (2002) 236–243.
[2] D.L. Black, Mechanisms of alternative pre-messenger RNA splicing, Annu. Rev. Biochem. 72 (2003) 291–336.
[3] B.R. Graveley, Alternative splicing: increasing diversity in the proteomic world, Trends Genet. 17 (2001) 100–107.
[4] G. Yeo, D. Holste, G. Kreiman, C.B. Burge, Variation in alternative splicing across human tissues, Genome Biol. 5 (2004) R74.
[5] P.J. Grabowski, Genetic evidence for a Nova regulator of alternative splicing in the brain, Neuron 25 (2000) 254–256.
[6] D. Feng, J. Xie, Aberrant splicing in neurological diseases, Wiley Interdiscip. Rev. RNA 4 (2013) 631–649.
[7] R.K. Singh, T.A. Cooper, Pre-mRNA splicing in disease and therapeutics, Trends Mol. Med. 18 (2012) 472–482.
[8] K. Ancelin, U.C. Lange, P. Hajkova, R. Schneider, A.J. Bannister, T. Kouzarides, M.A. Surani, Blimp1 associates with Prmt5 and directs histone arginine methylation in mouse germ cells, Nat. Cell Biol. 8 (2006) 623–630.

[9] S. Majumder, L. Alinari, S. Roy, T. Miller, J. Datta, S. Sif, R. Baiocchi, S.T. Jacob, Methylation of histone H3 and H4 by PRMT5 regulates ribosomal RNA gene transcription, J. Cell. Biochem. 109 (2010) 553–563.

[10] W.W. Tee, M. Pardo, T.W. Theunissen, L. Yu, J.S. Choudhary, P. Hajkova, M.A. Surani, Prmt5 is essential for early mouse development and acts in the cytoplasm to maintain ES cell pluripotency, Genes Dev. 24 (2010) 2772–2777.

[11] G. Meister, C. Eggert, D. Buhler, H. Brahms, C. Kambach, U. Fischer, Methylation of Sm proteins by a complex containing PRMT5 and the putative U snRNP assembly factor pICln, Curr. Biol. 11 (2001) 1990–1994.

[12] M.A. Powers, M.M. Fay, R.E. Factor, A.L. Welm, K.S. Ullman, Protein arginine methyltransferase 5 accelerates tumor growth by arginine methylation of the tumor suppressor programmed cell death 4, Cancer Res. 71 (2011) 5579–5587.

[13] M. Jansson, S.T. Durant, E.C. Cho, S. Sheahan, M. Edelmann, B. Kessler, N.B. La Thangue, Arginine methylation regulates the p53 response, Nat. Cell Biol. 10 (2008) 1431–1439.

[14] Y.T. Kwak, J. Guo, S. Prajapati, K.J. Park, R.M. Surabhi, B. Miller, P. Gehrig, R.B. Gaynor, Methylation of SPT5 regulates its interaction with RNA polymerase II and transcriptional elongation properties, Mol. Cell 11 (2003) 1055–1066.

[15] M. Bezzi, S.X. Teo, J. Muller, W.C. Mok, S.K. Sahu, L.A. Vardy, Z.Q. Bonday, E. Guccione, Regulation of constitutive and alternative splicing by PRMT5 reveals a role for Mdm4 pre-mRNA in sensing defects in the spliceosomal machinery, Genes Dev. 27 (2013) 1903–1916.

[16] G. Nagamatsu, T. Kosaka, M. Kawasumi, T. Kinoshita, K. Takubo, H. Akiyama, T. Sudo, T. Kobayashi, M. Oya, T. Suda, A germ cell-specific gene, Prmt5, works in somatic cell reprogramming, J. Biol. Chem. 286 (2011) 10641–10648.

[17] M.E. Torres-Padilla, D.E. Parfitt, T. Kouzarides, M. Zernicka-Goetz, Histone arginine methylation regulates pluripotency in the early mouse embryo, Nature 445 (2007) 214–218.

[18] T.Y. Wei, C.C. Juan, J.Y. Hisa, L.J. Su, Y.C. Lee, H.Y. Chou, J.M. Chen, Y.C. Wu, S.C. Chiu, C.P. Hsu, K.L. Liu, C.T. Yu, Protein arginine methyltransferase 5 is a potential oncoprotein that upregulates G1 cyclins/cyclin-dependent kinases and the phosphoinositide 3-kinase/AKT signaling cascade, Cancer Sci. 103 (2012) 1640–1650.

[19] A. Scoumanne, J. Zhang, X. Chen, PRMT5 is required for cell-cycle progression and p53 tumor suppressor function, Nucleic Acids Res. 37 (2009) 4965–4976.

[20] Z. Zhou, X. Sun, Z. Zou, L. Sun, T. Zhang, S. Guo, Y. Wen, L. Liu, Y. Wang, J. Qin, L. Li, W. Gong, S. Bao, PRMT5 regulates Golgi apparatus structure through methylation of the golgin GM130, Cell Res. 20 (2010) 1023–1033.

[21] N. Cabrera-Poch, R. Pepperkok, D.T. Shima, Inheritance of the mammalian Golgi apparatus during the cell cycle, Biochim. Biophys. Acta 1404 (1998) 139–151.

[22] H. Stanley, J. Botas, V. Malhotra, The mechanism of Golgi segregation during mitosis is cell type-specific, Proc. Natl. Acad. Sci. U. S. A. 94 (1997) 14467–14470.

[23] D. Corda, M.L. Barretta, R.I. Cervigni, A. Colanzi, Golgi complex fragmentation in G2/M transition: an organelle-based cell-cycle checkpoint, IUBMB Life 64 (2012) 661–670.

[24] M. Sohail, W. Cao, N. Mahmood, M. Myschyshyn, S.P. Hong, J. Xie, Evolutionarily emerged G tracts between the polypyrimidine tract and 3′ AG are splicing silencers enriched in genes involved in cancer, BMC Genomics 15 (2014) 1143.

[25] M. Sohail, J. Xie, Evolutionary emergence of a novel splice variant with an opposite effect on the cell cycle, Mol. Cell. Biol. 35 (2015) 2203–2214.

[26] J. Xie, D.L. Black, A CaMK IV responsive RNA element mediates depolarization-induced alternative splicing of ion channels, Nature 410 (2001) 936–939.

[27] T. Pontinen, A. Melin, G. Varadi, K. Khanmoradi, D. Chewaproug, S.K. Kung, R. Zaki, J. Ortiz, Cutaneous metastasis of pancreatic adenocarcinoma after kidney transplant: a case report and review of the literature, Exp. Clin. Transplant. 8 (2010) 273–276.

[28] J. Yu, Y. Hai, G. Liu, T. Fang, S.K. Kung, J. Xie, The heterogeneous nuclear ribonucleoprotein L is an essential component in the Ca^{2+}/calmodulin-dependent protein kinase IV-regulated alternative splicing through cytidine-adenosine repeats, J. Biol. Chem. 284 (2009) 1505–1513.

[29] L. Li, S. Wang, A. Jezierski, L. Moalim-Nour, K. Mohib, R.J. Parks, S.F. Retta, L. Wang, A unique interplay between Rap1 and E-cadherin in the endocytic pathway regulates self-renewal of human embryonic stem cells, Stem Cells 28 (2010) 247–257.

[30] M. Mitui, S.A. Nahas, L.T. Du, Z. Yang, C.H. Lai, K. Nakamura, S. Arroyo, S. Scott, A. Purayidom, P. Concannon, M. Lavin, R.A. Gatti, Functional and computational assessment of missense variants in the ataxia-telangiectasia mutated (ATM) gene: mutations with increased cancer risk, Hum. Mutat. 30 (2009) 12–21.

[31] D.P. Hill, K.A. Robertson, Differentiation of LA-N-5 neuroblastoma cells into cholinergic neurons: methods for differentiation, immunohistochemistry and reporter gene introduction, Brain Res. Brain Res. Protoc. 2 (1998) 183–190.

[32] J.C. Pence, N.A. Shorter, In vitro differentiation of human neuroblastoma cells caused by vasoactive intestinal peptide, Cancer Res. 50 (1990) 5177–5183.

[33] C.J. Thiele, P.S. Cohen, M.A. Israel, Regulation of c-myb expression in human neuroblastoma cells during retinoic acid-induced differentiation, Mol. Cell. Biol. 8 (1988) 1677–1683.

[34] L. Zhang, M. Procuik, T. Fang, S.K. Kung, Functional analysis of the quantitative expression of a costimulatory molecule on dendritic cells using lentiviral vector-mediated RNA interference, J. Immunol. Methods 344 (2009) 87–97.

[35] D.S. An, S.K. Kung, A. Bonifacino, R.P. Wersto, M.E. Metzger, B.A. Agricola, S.H. Mao, I.S. Chen, R.E. Donahue, Lentivirus vector-mediated hematopoietic stem cell gene transfer of common gamma-chain cytokine receptor in rhesus macaques, J. Virol. 75 (2001) 3547–3555.

[36] S. Ma, G. Liu, Y. Sun, J. Xie, Relocalization of the polypyrimidine tract-binding protein during PKA-induced neurite growth, Biochim. Biophys. Acta 1773 (2007) 912–923.

[37] G. Liu, A. Razanau, Y. Hai, J. Yu, M. Sohail, V.G. Lobo, J. Chu, S.K. Kung, J. Xie, A conserved serine of heterogeneous nuclear ribonucleoprotein L (hnRNP L) mediates depolarization-regulated alternative splicing of potassium channels, J. Biol. Chem. 287 (2012) 22709–22716.

[38] M.D. Robinson, D.J. McCarthy, G.K. Smyth, EdgeR: a bioconductor package for differential expression analysis of digital gene expression data, Bioinformatics 26 (2010) 139–140.

[39] S. Anders, W. Huber, Differential expression analysis for sequence count data, Genome Biol. 11 (2010) R106.

[40] W. Huang da, B.T. Sherman, R.A. Lempicki, Systematic and integrative analysis of large gene lists using DAVID bioinformatics resources, Nat. Protoc. 4 (2009) 44–57.

[41] W. Huang da, B.T. Sherman, R.A. Lempicki, Bioinformatics enrichment tools: paths toward the comprehensive functional analysis of large gene lists, Nucleic Acids Res. 37 (2009) 1–13.

[42] A. Colanzi, C. Hidalgo Carcedo, A. Persico, C. Cericola, G. Turacchio, M. Bonazzi, A. Luini, D. Corda, The Golgi mitotic checkpoint is controlled by BARS-dependent fission of the Golgi ribbon into separate stacks in G2, EMBO J. 26 (2007) 2465–2476.

[43] D. Tang, Y. Wang, Cell cycle regulation of Golgi membrane dynamics, Trends Cell Biol. 23 (2013) 296–304.

[44] X. Su, C. Qian, Q. Zhang, J. Hou, Y. Gu, Y. Han, Y. Chen, M. Jiang, X. Cao, miRNomes of haematopoietic stem cells and dendritic cells identify miR-30b as a regulator of Notch1, Nat. Commun. 4 (2013) 2903.

[45] K.Y. King, M.A. Goodell, Inflammatory modulation of HSCs: viewing the HSC as a foundation for the immune response, Nat. Rev. Immunol. 11 (2011) 685–692.

[46] C. Auffray, M.H. Sieweke, F. Geissmann, Blood monocytes: development, heterogeneity, and relationship with dendritic cells, Annu. Rev. Immunol. 27 (2009) 669–692.

[47] A. Kumanogoh, K. Suzuki, E. Ch'ng, C. Watanabe, S. Marukawa, N. Takegahara, I. Ishida, T. Sato, S. Habu, K. Yoshida, W. Shi, H. Kikutani, Requirement for the lymphocyte semaphorin, CD100, in the induction of antigen-specific T cells and the maturation of dendritic cells, J. Immunol. 169 (2002) 1175–1181.

[48] H. Takamatsu, N. Takegahara, Y. Nakagawa, M. Tomura, M. Taniguchi, R.H. Friedel, H. Rayburn, M. Tessier-Lavigne, Y. Yoshida, T. Okuno, M. Mizui, S. Kang, S. Nojima, T. Tsujimura, Y. Nakatsuji, I. Katayama, T. Toyofuku, H. Kikutani, A. Kumanogoh, Semaphorins guide the entry of dendritic cells into the lymphatics by activating myosin II, Nat. Immunol. 11 (2010) 594–600.

[49] Q. Zhao, G. Rank, Y.T. Tan, H. Li, R.L. Moritz, R.J. Simpson, L. Cerruti, D.J. Curtis, D.J. Patel, C.D. Allis, J.M. Cunningham, S.M. Jane, PRMT5-mediated methylation of histone H4R3 recruits DNMT3A, coupling histone and DNA methylation in gene silencing, Nat. Struct. Mol. Biol. 16 (2009) 304–311.

[50] N. Stopa, J.E. Krebs, D. Shechter, The PRMT5 arginine methyltransferase: many roles in development, cancer and beyond, Cell. Mol. Life Sci. 72 (2015) 2041–2059.

[51] M.C. Ho, C. Wilczek, J.B. Bonanno, L. Xing, J. Seznec, T. Matsui, L.G. Carter, T. Onikubo, P.R. Kumar, M.K. Chan, M. Brenowitz, R.H. Cheng, U. Reimer, S.C. Almo, D. Shechter, Structure of the arginine methyltransferase PRMT5-MEP50 reveals a mechanism for substrate specificity, PLoS One 8 (2013) e57008.

[52] S. Antonysamy, Z. Bonday, R.M. Campbell, B. Doyle, Z. Druzina, T. Gheyi, B. Han, L.N. Jungheim, Y. Qian, C. Rauch, M. Russell, J.M. Sauder, S.R. Wasserman, K. Weichert, F.S. Willard, A. Zhang, S. Emtage, Crystal structure of the human PRMT5:MEP50 complex, Proc. Natl. Acad. Sci. U. S. A. 109 (2012) 17960–17965.

[53] K. Furuno, T. Masatsugu, M. Sonoda, T. Sasazuki, K. Yamamoto, Association of polycomb group SUZ12 with WD-repeat protein MEP50 that binds to histone H2A selectively in vitro, Biochem. Biophys. Res. Commun. 345 (2006) 1051–1058.

[54] L. Sun, M. Wang, Z. Lv, N. Yang, Y. Liu, S. Bao, W. Gong, R.M. Xu, Structural insights into protein arginine symmetric dimethylation by PRMT5, Proc. Natl. Acad. Sci. U. S. A. 108 (2011) 20538–20543.

[55] G. Guderian, C. Peter, J. Wiesner, A. Sickmann, K. Schulze-Osthoff, U. Fischer, M. Grimmler, RioK1, a new interactor of protein arginine methyltransferase 5 (PRMT5), competes with pICln for binding and modulates PRMT5 complex composition and substrate specificity, J. Biol. Chem. 286 (2011) 1976–1986.

[56] B. Gurung, Z. Feng, D.V. Iwamoto, A. Thiel, G. Jin, C.M. Fan, J.M. Ng, T. Curran, X. Hua, Menin epigenetically represses Hedgehog signaling in MEN1 tumor syndrome, Cancer Res. 73 (2013) 2650–2658.

[57] Z. Gu, Y. Li, P. Lee, T. Liu, C. Wan, Z. Wang, Protein arginine methyltransferase 5 functions in opposite ways in the cytoplasm and nucleus of prostate cancer cells, PLoS One 7 (2012) e44033.

[58] D. Eckert, K. Biermann, D. Nettersheim, A.J. Gillis, K. Steger, H.M. Jack, A.M. Muller, L.H. Looijenga, H. Schorle, Expression of BLIMP1/PRMT5 and concurrent histone H2A/H4 arginine 3 dimethylation in fetal germ cells, CIS/IGCNU and germ cell tumors, BMC Dev. Biol. 8 (2008) 106.

[59] I. Goulet, G. Gauvin, S. Boisvenue, J. Cote, Alternative splicing yields protein arginine methyltransferase 1 isoforms with distinct activity, substrate specificity, and subcellular localization, J. Biol. Chem. 282 (2007) 33009–33021.

[60] C. Nicholas, J. Yang, S.B. Peters, M.A. Bill, R.A. Baiocchi, F. Yan, S. Sif, S. Tae, E. Gaudio, X. Wu, M.R. Grever, G.S. Young, G.B. Lesinski, PRMT5 is upregulated in malignant and metastatic melanoma and regulates expression of MITF and p27(Kip1.), PLoS One 8 (2013) e74710.

[61] K. Shilo, X. Wu, S. Sharma, M. Welliver, W. Duan, M. Villalona-Calero, J. Fukuoka, S. Sif, R. Baiocchi, C.L. Hitchcock, W. Zhao, G.A. Otterson, Cellular localization of protein arginine methyltransferase-5 correlates with grade of lung tumors, Diagn. Pathol. 8 (2013) 201.

[62] C.M. Koh, M. Bezzi, E. Guccione, The where and the how of PRMT5, Curr. Mol. Biol. Rep. 1 (2015) 19–28.

[63] A.F. Bruns, C. Grothe, P. Claus, Fibroblast growth factor 2 (FGF-2) is a novel substrate for arginine methylation by PRMT5, Biol. Chem. 390 (2009) 59–65.

[64] S. Massenet, L. Pellizzoni, S. Paushkin, I.W. Mattaj, G. Dreyfuss, The SMN complex is associated with snRNPs throughout their cytoplasmic assembly pathway, Mol. Cell. Biol. 22 (2002) 6533–6541.